Biochemical Journal Immediate Publication. Published on 13 May 2004 as manuscript BJ20040302

Mutational analysis of the triclosan-binding region of enoyl-ACP reductase from *Plasmodium falciparum*

Mili Kapoor[†], Jayashree Gopalakrishnapai[†], Namita Surolia[#], Avadhesha Surolia[†]*

[†]Molecular Biophysics Unit, Indian Institute of Science, Bangalore-560012, India

[#]Molecular Biology and Genetics Unit, Jawaharlal Nehru Centre for Advanced Scientific Research, Jakkur, Bangalore, India

*Corresponding author
Prof. Avadhesha Surolia
Molecular Biophysics Unit
Indian Institute of Science
Bangalore-560012, INDIA
Phone: 91-80-22932714
Fax: 91-80-23600535
E-mail: surolia@mbu.iisc.ernet.in.

Biochemical Journal Immediate Publication. Published on 13 May 2004 as manuscript BJ20040302

SYNOPSIS

Triclosan, a known antibacterial acts by inhibiting enoyl-ACP reductase (ENR), a key enzyme of the type II fatty acid synthesis (FAS) system. *Plasmodium falciparum,* the human malaria-causing parasite harbors the type II FAS, in contrast to its human host, which utilizes type I FAS. Due to this striking difference, enoyl-ACP reductase has emerged as an important target for the development of new antimalarials. Modeling studies and the crystal structure of *P. falciparum* ENR have highlighted the features of ternary complex formation between the enzyme, triclosan and NAD^+ (Suguna, K. et al., *Biochem. Biophys. Res. Commun.* 283, 224-228; Perozzo, R. et al., *J. Biol. Chem.* **277**, 13106-13114 and Swarnamukhi et al., PDB:1UH5). To address the issue of the importance of the residues involved in strong, specific and stoichiometric binding of triclosan to *P. falciparum* ENR, we mutated the following residues: Ala-217, Asn-218, Met-281, and Phe-368. The affinity of all the mutants was reduced for triclosan as compared to the wild-type enzyme to different extents. The most significant mutation was A217V, which led to a greater than 7000-fold decrease in the binding affinity for triclosan as compared to wild-type PfENR. A217G showed only 10-fold reduction in the binding affinity. These studies thus point out significant differences in the triclosan binding region of the *P. falciparum* enzyme from those of its bacterial counterparts.

RUNNING TITLE: Site-specific mutants of *P. falciparum* enoyl-ACP reductase.

KEY WORDS: Enoyl-ACP reductase, FabI, triclosan, mutants, inhibitor, Fatty acid biosynthesis

ABBREVIATIONS: FAS: Fatty acid biosynthesis; FabI/ENR: Enoyl-ACP reductase; PfENR: *Plasmodium falciparum* Enoyl-ACP reductase

Biochemical Journal Immediate Publication. Published on 13 May 2004 as manuscript BJ20040302

INTRODUCTION

The human malaria causing parasite, *Plasmodium falciparum* has been shown to harbor type II fatty acid biosynthesis enzymes, in contrast to its human host that synthesizes fatty acids *via* the type I pathway [1, 2]. The realization that the fatty acid biosynthesis pathway of the malaria parasite could be a potential target of antimalarials, has led to renewed research in this area, as apparent from the recent research and review articles published [1, 3-8]. Triclosan has been shown to be effective against a broad spectrum of bacteria including *E. coli* [9], *S. aureus* [10] and *M. smegmatis* [11]. Triclosan was found to inhibit the growth of *P. falciparum* in red blood cell cultures with an IC_{50} of 0.7 μM and its efficacy demonstrated in a mouse model of *P. berghei* [1].

It was shown earlier that triclosan blocks lipid synthesis in *E. coli* and mutations in enoyl-ACP reductase prevent this blockage [9]. A series of *E. coli* mutants were isolated that were resistant to triclosan. The MIC ratio of the various mutants with respect to the wild-type was calculated as 95 (G93V), 12.2 (M159T) and 6.1 (F203L). Enoyl-ACP reductase, catalyzing the last step in the elongation cycle of fatty acid biosynthesis, reduces a carbon-carbon double bond in an enoyl moiety that is covalently linked to an acyl carrier protein. The enzyme has been studied from various sources [1, 6-8, 11-15]. The recent investigation into the mechanism of triclosan inhibition and selectivity in *E. coli* FabI, in which three mutations were characterized namely G93V, M159T and F203L correlate well with the MIC data [9, 14]. Also, the mutation of Gly-93 to Ser leads to diazaborine resistance, while the mutation of the analogous residue in InhA (S94A) leads to isoniazid resistance [16]. These results also correlate with the crystal data of *E. coli* FabI protein, which shows that all the three residues line a cleft at which NADH binds [15].

In *P. falciparum* ENR, alanine is present at the place corresponding to Gly-93. The other two residues (M159 and F203) are conserved. Thus, the residues in PfENR corresponding to Gly-93, Met-159 and Phe-203 of *E. coli* FabI are Ala-217, Met-281 and Phe-368. On the basis of modeling studies, the residues Ala-217, Met-281 and Phe-368 were implicated in triclosan binding [6]. Consistent with the above observations, the crystal structure of PfENR solved with NAD^+ and triclosan demonstrated that the mode of triclosan binding was very similar to that observed in *E. coli*-NAD^+-triclosan complex [8]. The residues Ala-217, Asn-218, Met-281 and Phe-368 are present close to the triclosan binding site of PfENR. Hence, to characterize the role

played by these residues of *P. falciparum* ENR in triclosan binding, we generated the following mutants: A217V, A217G, N218A, N218D, M281A, M281T, F368A and F368I.

The mutants were expressed, purified by Ni-NTA affinity chromatography and characterized by determining the kinetic constants for their binding to substrates and the inhibitor, triclosan. The study reports that as in the case of *E. coli* FabI, substitution of Ala-217 by an amino acid with a bulkier side chain is not tolerated for triclosan binding. The other mutant enzymes also have reduced affinity for triclosan probably due to abrogation of important contacts between the side chains of the amino acids and triclosan.

MATERIALS AND METHODS

Materials

Media components were obtained from Hi-media (Delhi, India). β-NADH, β-NAD^+, crotonoyl-CoA, imidazole and SDS-PAGE reagents were obtained from Sigma Chemical Co., St. Louis, MO. Triclosan was obtained from Kumar organic products (Bangalore, India). His-bind resin and anti-His tag antibody were obtained from Novagen (Madison, USA). Protein molecular weight marker was obtained from MBI (Fermentas Inc., USA). Anti-mouse rabbit antibody and prestained molecular weight marker were obtained from Bangalore Genei (Bangalore, India). All other chemicals used were of analytical grade.

Strains and plasmids

E. coli DH5α cells were used during the cloning of the mutants. pET-28a(+) vector (Novagen) and BL21 (DE3) cells (Novagen) were used for the expression of mutant PfENRs. Primers for constructing the mutants were obtained from Sigma.

Construction of A217V, A217G, N218A, N218D, F368A and F368I mutants

The single point mutants of Ala-217 to Val (A217V), Ala-217 to Gly (A217G), Asn-218 to Ala (N218A), Asn-218 to Asp (N218D), Phe-368 to Ala (F368A) and Phe-368 to Ile (F368I) were generated by PCR overlap extension method. A pET 28a(+)-derived vector [7] containing the sequence of *pfenr* (GenBank accession number AF332608) was used as the template plasmid for all the reactions. For making the A217V mutant, the two PCR products with overlapping ends were generated by using the “PlasF” primer together with “A217VF” and “A217R” together with “PlasR”. The PCR cycles used were: 1 x {95º C, 3 min}; 25 x {95º C, 1 min, 50º, 1 min, 72º C, 1 min}; 1 x {72º C, 7 min}. The combined PCR product was digested with NcoI and BamHI and

cloned into pET28a(+) digested with the same enzymes. A217G, N218A, N218D, F368A and F368I were generated in a similar manner using the primers listed in Table 1. The correct sequences of all constructs were verified by DNA sequencing.

Construction of M281A and M281T mutants

M281A mutant was generated by amplification of the wild-type *pfenr* plasmid using M281AF and M281AR primers. The PCR cycles used were: 1 x {95º C, 3 min}; 19 x {95º C, 1 min, 62º, 1 min, 72º C, 6 min 30 sec}; 1 x {72º C, 7 min}. The PCR product was digested with DpnI and transformed into *E. coli* DH5α cells. The colonies were screened by digesting with XhoI as the primers lead to a silent mutation in *pfenr* leading to the generation of XhoI site. M281T mutant was generated in a similar manner using the primers listed in Table 1. The correct sequences was verified by DNA sequencing.

Overexpression and purification of wild-type and mutant PfENRs

Wild-type and mutant PfENRs were expressed and purified as described earlier [7]. Briefly, the plasmid containing *pfenr* was transformed in BL21(DE3) cells. Cultures were grown at 37 ºC for 12 hrs., pelleted and resuspended in 20 mM Tris-Cl buffer containing, 500 mM NaCl and 5 mM imidazole, pH 7.4. The cultures were lysed by sonication followed by purification of the His-tagged PfENR on Ni-NTA agarose column using an imidazole gradient. PfENR eluted at 400 mM imidazole concentration. The purity of the protein was confirmed by 10% SDS-PAGE. The fractions containing pure protein were pooled and concentrated using 10 kDa centripreps (Amicon) for further experiments. The pET 28a(+) constructs harboring the mutated *pfenr* sequences were transformed into BL21(DE3) cells and the mutant proteins purified using the same protocol as mentioned for the wild-type PfENR. E_{280} of mutant ENRs was estimated using the ProtParam tool at http://tw.expasy.org/tools/protparam.html.

Enzyme assay

All experiments were carried out on a Jasco V-530 UV-Vis spectrophotometer. Enoyl-ACP reductase was assayed at 25 °C by monitoring the decrease in A_{340} due to the oxidation of NADH using crotonoyl-CoA as a substrate [7]. The standard reaction mixture in a total volume of 100 µl contained 20 mM Tris-Cl buffer pH 7.4, 500 mM NaCl, 100 µM crotonoyl-CoA and 100 µM NADH. The K_m for each substrate was determined by varying the concentrations of that substrate while keeping the concentration of the other substrate constant. The kinetic parameters

were obtained by fitting initial velocity data to Michaelis-Menten equation by non-linear regression analysis using GraphPad Prism software.

Enzyme inhibition studies

The inhibition of PfENR activity was monitored by the spectrophotometric assay performed as described above except that triclosan was added prior to the initiation of the reaction by addition of crotonoyl-CoA. The studies were performed in the presence of 1% DMSO used for solubilizing the inhibitors. In order to study the inhibition of ENR by triclosan by steady state approach, a modified protocol was followed as described in [17]. Enoyl-ACP reductase was preincubated with the respective inhibitor and various concentrations of the coenzymes at 4 °C for 5 hours. This was warmed to 25 °C and assay started by the addition of crotonoyl-CoA. The mechanism of inhibition was identified by studying the dependence of the apparent inhibition constant (K_i') on the substrate concentration. The K_i' was determined using the equation:

$$v = v_o/(1+[I]/ K_i') \quad (1)$$

where v_o is the uninhibited rate and v is the rate in the presence of the inhibitor.

The substrate dependence of K_i' for competitive, uncompetitive and mixed noncompetitive kinetics is defined by equations 2, 3 and 4 respectively.

$$K_i' = K_{is}([S]+K_m)/K_m \quad (2)$$

$$K_i' = K_{ii}([S]+K_m)/[S] \quad (3)$$

$$K_i' = K_{is}K_{ii}([S]+K_m)/(K_{is}[S]+K_{ii}K_m) \quad (4)$$

RESULTS

We have previously demonstrated the inhibition of *P. falciparum* ENR by the well-known antibacterial, triclosan and determined the inhibition constants for the same [1, 7]. Here, we have examined the effect of mutations that span the triclosan binding region, on the affinity of triclosan as well as its substrate binding and enzymatic activity.

Expression and purification of wild-type and mutant ENR

Wild-type and mutant ENRs were purified as described previously [7]. The mobility of the mutant proteins as analyzed by SDS-PAGE was similar to the wild-type protein (supplementary data). The expression of the recombinant His-tagged wild-type and mutant ENR was also analyzed using anti-His antibody and a band corresponding to the position of band in SDS-PAGE was obtained (supplementary data). The expected molecular mass of ENR as calculated

using the ProtParam tool at http://kr.expasy.org/tools/ was Mr 38166. The molecular weight of purified ENR was further confirmed by MALDI mass spectrometry to Mr 38163 (±2) Da. The molecular weights of the mutant ENRs were also confirmed by MALDI and were found to be of the expected molecular masses.

Gel filtration and circular dichroism analyses of the mutants

Changes in the overall shape or the quaternary structure of the molecule potentially introduced by mutagenesis was first probed using size exclusion chromatography. Wild-type PfENR elutes as a single peak at a volume of 7.6 ml on a Superdex-200 gel-filtration column (supplementary data). The mutants eluted at the same volume as their wild type counterpart. The elution positions of the wild-type and mutants of PfENR correspond to a relative molecular weight of 150 (±10) kDa indicating the enzymes to be a homotetramer and that the mutations did not alter the overall shape or the quaternary structure of PfENR. CD spectroscopy was used to investigate potential perturbations in the secondary and tertiary structure of PfENR mutants, which indicated that the various amino acid substitutions had no effect on the overall folding of the resultant mutant protein (supplementary data).

Kinetic analysis of the mutants

As can be seen in Table 2, the kinetic constants (K_m and k_{cat}) for A217V, A217G, M281A, M281T, F368A and F368I remain unchanged with respect to the wild-type ENR. Thus, the mutations do not affect the catalytic efficiency of the enzyme. Interestingly, N218A and N218D mutants had an increase in the K_m for NADH as compared to the wild-type. The K_m value of wild-type PfENR for NADH was calculated earlier as 33 μM [7]. N218A and N218D had a K_m value 73 μM and 100 μM respectively. Such a change for the *E. coli* enzyme has not been observed.

Inhibition constants of wild-type and mutant PfENR

Earlier studies on the *E. coli* and *Staphylococcus aureus* FabI have shown that triclosan forms a ternary complex with NAD^+, the oxidized co-factor [16, 18-21]. Moreover, a ternary complex formation between ENR from *P. falciparum*, triclosan and NAD^+ was also demonstrated in our earlier studies [1, 7]. These observations were confirmed by the crystal structure of PfENR [8]. Both our modeling studies and the crystal structure of the ternary complex of PfENR with triclosan and NAD^+, show that the ring A of triclosan in addition to interacting face-to-face with the nicotinamide ring of NAD^+, also makes additional van der Waals interactions with certain

PfENR residues including Phe-368 [6, 8]. Ring B is located in a pocket bounded by pyrophosphate and nicotinamide moieties of NAD^+, by the peptide backbone residues 217-231 and by the side chains of Asn-218, Val-222, Tyr-277 and Met-281 (Fig. 1). In order to analyze the contribution of these residues towards triclosan binding, we mutated key residues that interact with the ring A and B of triclosan. Also, mutations in these residues have been found to confer resistance to *E. coli* FabI towards triclosan.

The value of Ki' for the inhibition of different mutants by triclosan with respect to NAD^+ was estimated in the presence of 250 μM NADH and varying concentrations of NAD^+. The curve was fitted to competitive, uncompetitive and noncompetitive inhibition using equations 2, 3 and 4. The inhibition constants of triclosan with respect to the different mutants are shown in Table 3.

Residues interacting with Ring B of triclosan

The K_i of triclosan for A217V (232 (±5) nM) is far greater than the wild-type PfENR (0.03 (± 0.001) nM), demonstrating its low affinity for A217V (Figure 2A). The A217G PfENR mutant also showed lower affinity towards triclosan as compared to the wild-type ENR with a K_i of 0.57 (±0.05) nM (Figure 2B). N218A and N218D had a K_i of 2.1 (±0.1) and 1.5 (±0.04) nM, respectively. M281A and M281T had a K_i of 9.34 (±0.81) and 10.0 (±0.89) nM, respectively. A plot of K_i *versus* different concentrations of NAD^+ is shown as Figure 2A and B for two representative examples, A217V and A217G. In all the cases the curve fits well to uncompetitive kinetics demonstrating the preference of triclosan for binding to PfENR as well as its mutant counterparts in the presence of NAD^+.

Residues interacting with Ring A of triclosan

A K_i of 7.2 (±0.9) and 6.3 (±0.56) nM was obtained for F368A and F368I PfENR mutants, respectively while that for its wild-type counterpart was found to be 0.03 nM implying the importance of this interaction for binding of triclosan to PfENR.

DISCUSSION

Triclosan inhibits enoyl-ACP reductase (one of the enzymes of the FAS pathway) from *E. coli* and *P. falciparum* very potently. However, its affinity for the enzyme from *M. tuberculosis* is 10,000 fold lower [22]. Also, another diphenyl ether, 2-2' dihydroxydiphenyl ether, inhibits the enzyme from *E. coli* 1000 fold more potently as compared to the *P. falciparum* enzyme [1, 7].

The crystal structures of enoyl-ACP reductase (FabI) from *E. coli* [19-21], *M. tuberculosis* [13] and *P. falciparum* [8] are now available. Yet, the reasons for such large differences in the binding affinities are still not clear. Thus, stressing the need to understand the structural features that govern such differences in the affinities of the enzyme from different sources. Multiple sequence alignment of ENR from different organisms comparing the *P. falciparum* ENR with its counterparts from other organisms is shown in Figure 3. In this paper, we have taken a mutational approach to study the triclosan binding site of ENR from *P. falciparum*, which highlights the subtle differences in the binding site of PfENR as compared to enoyl-ACP reductases from other sources. Thus, the knowledge of these differences would help in the design of potent inhibitors of FabI.

The role of a particular amino acid residue of a protein towards interaction with a ligand can be judged by site-directed mutagenesis. Hence, we performed a series of mutations spanning the triclosan binding site of ENR. The expression of recombinant ENR-His tagged fusion protein and the purification of the ENR was confirmed by using anti-His antibody. To exclude the possibility that the triclosan binding to mutant ENRs was decreased due to the introduction of gross structural changes, we first analyzed the oligomerization status and conformation of wild-type and mutant ENR by gel-filtration and circular dichroism (CD) spectroscopy (supplementary data). Thereafter, we performed a thorough analysis of the binding of PfENR mutants to triclosan.

We had earlier demonstrated that triclosan acts as a potent inhibitor of *P. falciparum* ENR [7]. As the concentration of NAD^+ increases during the course of the reaction catalyzed by ENR and since NAD^+ potentiates inhibition of ENR by triclosan, a modified protocol was followed. The reaction mixtures containing NAD^+ were preincubated for 5 hrs. at 4 ºC in order to achieve a steady-state before starting the assay. Also, this would mean that the concentration of NAD^+ does not change significantly during the course of assay [17]. Triclosan demonstrated uncompetitive kinetics with an inhibition constant of 0.03 nM at saturating NAD^+ concentration, demonstrating that triclosan binds to the enzyme-NAD^+ complex with far greater affinity compared to the enzyme alone [7]. Indeed an increase in the binding constant of triclosan towards PfENR in the presence of NAD^+ has been observed in surface plasmon resonance experiments (Kapoor et al., accompanying paper).

Single amino acid substitutions (G93V, M159T and F203L) in the sequence of *E. coli* FabI have been shown to confer resistance to triclosan [9]. The structure of the *E. coli*-NAD^+-triclosan complex revealed that these residues make direct contacts with triclosan. The mutation of Gly-93 to Val specifically led to a 100 fold decrease in the MIC, which can be attributed to the steric contacts between the side chains of Val and triclosan [9, 14, 22]. This is also the site for G93A/S/C/V *E. coli* mutants resistant to diazaborine, again through the introduction of adverse steric contacts [15]. Although, the *Mycobacterium smegmatis* InhA mutant, S94A leads to triclosan resistance [11], the same mutation does not affect the affinity of triclosan for InhA from *Mycobacterium tuberculosis* [22]. Consistent with these observations, the mutation of Ala-217 to Val of *P. falciparum* ENR led to a dramatic decrease in the affinity of triclosan, as apparent from the value of inhibition constant (K_i) (Table 3). The *E. coli* mutant G93V showed 9000-fold reduced affinity for triclosan as compared to the wild-type FabI [14]. As can be seen in Figure 1, Ala-217 comes close to the 2,4-dichlorophenoxy ring (ring B) of triclosan. Thus, it seems reasonable to conclude that even in the case of PfENR, the mutation of Ala-217 to Val leads to unacceptable steric contacts between the side chain of Val and triclosan, leading to reduced affinity of triclosan for the enzyme. Interestingly enough, the substitution of Ala by a smaller amino acid Gly, also led to decreased affinity but to a limited extent. There was a 19-fold decrease in the inhibition constant of A217G mutant with respect to the wild-type. The 2-chloro atom of the ring B of triclosan is positioned close to the side chain of Ala-217 [6, 17]. The decrease in the affinity of A217G mutant for triclosan could be due to loss of contacts between triclosan and the side chain of alanine. In contrast, *E. coli* enzyme has a glycine at the corresponding position and its replacement by alanine reduced the affinity considerably for triclosan. Thus, despite having a nearly similar tertiary structure and the binding pocket, the malarial enzyme differs strikingly from its bacterial counterpart.

The mutation of Asn-218, Met-281 and Phe-368 also made the enzyme resistant towards triclosan, albeit to different extents. As illustrated in Figure 1, all three residues are located close to the inhibitor-binding site of the ternary complex of ENR-triclosan and NAD^+. The ring B of triclosan was located in a pocket interacting with pyrophosphate and nicotinamide moieties of NAD^+, by peptide backbone residues 217-231 and by side chains of Asn-218, Val-222, Tyr-277 and Met-281 [6]. The mutation of Asn-218 to Asp led to a 50-fold decrease in the affinity of the malarial enzyme for triclosan. The mutant M281T had 333-fold reduced affinity for triclosan.

This could be because of the loss of van der Waals contacts between the 4-chloro atom of ring B and hydrophobic side chain of Met-281 [6, 8]. In order to rule out the possibility that the addition of the beta-branched threonine could introduce indirect effects due to the perturbation of the local structure, M281A mutant was made, that showed K_i similar to M281T.

As observed from the crystal structure of the ternary complex of *P. falciparum* with triclosan and NAD^+, the ring A of triclosan makes van der Waals interactions with the side chain of Phe-368 [6]. Also, the 4-chloro atom of triclosan makes several van der Waals contact with Phe-368 [6, 17]. The mutation of Phe-368 to Ala and Ile led to 240 and 210-fold decrease in the affinity of enzyme for the inhibitor highlighting the importance of stacking and the van der Waals interactions between ring A of triclosan and Phe-368 of the enzyme.

Thus, to conclude the strong affinity of *P. falciparum* ENR for triclosan is compromised due to critical mutations at its active site. Because of the subtle but significant differences observed in these studies for the contribution of key residues to the binding affinity of PfENR for triclosan in contrast to its bacterial counterparts, it should be possible to design better and specific analogs of triclosan as antimalarial agents that spare the bacterial enzyme. Also, several point mutations reduced inhibitory potency of triclosan without affecting the catalytic properties of the enzyme, indicating that resistant strains could arise under the pressure of the biocide triclosan. Our findings thus hint to the need for the design and development of more effective inhibitors and more importantly their usage in combination therapies to ward off the emergence of drug resistance strains [23].

ACKNOWLEDGEMENTS

This work was supported by a grant from the Department of Biotechnology, Government of India to N.S and A.S.

REFERENCES

1) Surolia, N. and Surolia, A. (2001) Triclosan offers protection against blood stages of malaria by inhibiting enoyl-ACP reductase of *Plasmodium falciparum*. Nature Med. **7**, 167-173

2) Waller, R. F., Keeling, P. J., Donald, R. G. K., Striepen, B., Handman, E., Lang- Unnasch, N., Cowman, A. F., Besra, G. S., Roos, D. S. and McFadden, G. I. (1998) Nuclear-encoded proteins target to the plastid in *Toxoplasma gondii* and *Plasmodium falciparum*. Proc. Natl. Acad. Sci. USA. **95**, 12352-12357

3) Rao, S. P., Surolia, A. and Surolia, N. (2003) Triclosan: A shot in the arm for antimalarial chemotherapy. Mol. Cell Biochem. **253**, 55-63

4) Gornicki P. (2003) Apicoplast fatty acid biosynthesis as a target for medical intervention in apicomplexan parasites. Int. J. Parasitol. **33**, 885-896

5) Muralidharan, J., Suguna, K., Surolia, A. and Surolia, N. (2003) Exploring the interaction energies for the binding of hydroxydiphenyl ethers to enoyl-acyl carrier protein reductases. J. Biomol. Struct. Dyn. **20**, 589-594

6) Suguna, K., Surolia, A. and Surolia, N. (2001) Structural basis for triclosan and NAD binding to enoyl-ACP reductase of *Plasmodium falciparum*. Biochem. Biophys. Res. Commun. **283**, 224-228

7) Kapoor, M., Dar, M. J., Surolia, A. and Surolia, N. (2001) Kinetic determinants of the interaction of enoyl-ACP reductase from *Plasmodium falciparum* with its substrates and inhibitors. Biochem. Biophys. Res. Comm. **289**, 832-837

8) Perozzo, R., Kuo, M., Sidhu, A. S., Valiyaveettil, J. T., Bittman, R., Jacobs Jr., W. R., Fidock, D. A. and Sacchettini, J. C. (2002) Structural elucidation of the specificity of the antibacterial agent triclosan for malarial enoyl acyl carrier protein reductase. J. Biol.Chem. **277**, 13106-13114

9) McMurray, L. M., Oethinger, M. and Levy, S.B. (1998) Triclosan targets lipid synthesis. Nature **394**, 531-532

10) Fan, F., Yan, K., Wallis, N. G., Reed, S., Moore, T. D., Rittenhouse, S. F., DeWolf, W. E. Jr, Huang, J., McDevitt, D., Miller, W. H., Seefeld, M. A., Newlander, K. A., Jakas, D. R., Head, M. S. and Payne, D. J. (2002) Defining and combating the mechanisms of triclosan resistance in clinical isolates of *Staphylococcus aureus*. Antimicrob. Agents Chemother. **46**, 3343-3347

11) McMurry, L. M., McDermott, P. F. and Levy, S. B. (1999) Genetic evidence that InhA of *Mycobacterium smegmatis* is a target for triclosan. Antimicrob. Agents Chemother. **43**, 711-713

12) Bergler, H., Wallner, P., Ebeling, A., Leitinger, B., Fuchsbichler, S., Aschauer, H., Kollenz, G., Högenauer, G. and Turnowsky, F. (1994) Protein EnvM is the NADH-dependent enoyl-ACP reductase (FabI) of *Escherichia coli*. J. Biol. Chem. **269**, 5493-5496

13) Rafferty, J. B., Simon, J. W., Baldock, C., Artymiuk, P. J., Baker, P. J., Stuitje, A. R., Slabas, A. R. and Rice, D. W. (1995) Common themes in redox chemistry emerge from the X-ray structure of oilseed rape (*Brassica napus*) enoyl acyl carrier protein reductase. Structure **3**, 927-938

14) Sivaraman, S., Zwahlen, J., Bell, A. F., Hedstrom, L. and Tonge, P. J. (2003) Structure-activity studies of the inhibition of FabI, the enoyl reductase from *Escherichia coli*, by triclosan: Kinetic analysis of mutant FabIs. Biochemistry **42**, 4406-4413

15) Baldock, C., Rafferty, J. B., Stuitje, A. R., Slabas, A. R. and Rice, D. W. (1998) The X-ray structure of *Escherichia coli* enoyl reductase with bound NAD^+ at 2.1 Å resolution. J. Mol. Biol. **284**, 1529-1546

16) Dessen, A., Quemard, A., Blanchard, J. S., Jacobs Jr., W. R. and Sacchettini, J. C. (1995) Crystal structure and function of the isoniazid target of *Mycobacterium tuberculosis*. Science **267**, 1638-1641

17) Ward, W.H.J., Holdgate, G.A., Rowsell, S., Mclean, E., G., Pauptit, R.A., Clayton, E., Nichols, W.W., Colls, J.G., Minshull, C.A., Jude, D.A., Mistry, A., Timms, D., Camble, R., Hales, N.J., Britton, C.J. and Taylor, I.W.F. (1999) Kinetic and structural characteristics of the inhibition of enoyl (acyl carrier protein) reductase by triclosan. Biochemistry **38**, 12514-12525

18) Heath, R. J., Li, J., Roland, G. E. and Rock, C. O. (2000) Inhibition of the *Staphylococcus aureus* NADPH-dependent enoyl-acyl carrier protein reductase by triclosan and hexachlorophene. J. Biol. Chem. **275**, 4654–4659

19) Stewart, M. J., Parikh, S., Xiao, G., Tonge, P. J. and Kisker, C. (1999) Structural basis and mechanism of enoyl reductase inhibition by triclosan. J. Mol. Biol. **23**, 859-865

20) Roujeinikova, A., Levy, C. W., Rowsell, S., Sedelnikova, S., Baker, P. J., Minshull, C. A., Mistry, A., Colls, J. G., Camble, R., Stuitje, A. R., Slabas, A. R., Rafferty, J. B., Pauptit, R. A., Viner, R. and Rice, D. W. (1999) Crystallographic analysis of triclosan bound to enoyl reductase. J. Mol. Biol. **294**, 527-535

21) Levy, C. W., Roujeinikova, A., Sedelnikova, S., Baker, P. J., Stuitje, A. R., Slabas, A. R., Rice, D. W. and Rafferty, J. B. (1999) Molecular basis of triclosan activity. Nature **398**, 383-384

22) Parikh, S. L., Xiao, G. and Tonge, P. J. (2000) Inhibition of InhA, the enoyl reductase from *Mycobacterium tuberculosis*, by triclosan and isoniazid. Biochemistry **39**, 7645-7650

23) Ndyomugyenyi, R., Magnussen, P., Clarke, S. (2004) The efficacy of chloroquine, sulfadoxine-pyrimethamine and a combination of both for the treatment of uncomplicated *Plasmodium falciparum* malaria in an area of low transmission in western Uganda. Trop. Med. Int. Health. 9, 47-52.

24) Goodstadt, L. and Ponting, C. P. (2001) CHROMA: consensus-based colouring of multiple alignments for publication. Bioinformatics **17**, 845-846

Table 1

Overview of oligonucleotide primers used to generate the PfENR mutants.

Primer	Sequence
PlasF	5'-ACGTCCCATGGTGCATCATCATCATCATCATAATGAAGATATTTGTTTT ATTGCTGGTATAGG-3'
PlasR	5'-ATATGGATCCTCAATCATCTGGTAAAAACATTATATTTAATCCGTTATCC ACATATATTGTCTG-3'
A217GF	5'-CTCGTTCATTCTTTAGGCAACGCTAAAGAAGTTCAAAAAG-3'
A217GR	5'-CTTTTTGAACTTCTTTAGCGTTGCCTAAAGAATGAACGAG-3'
A217VF	5'-CTCGTTCATTCTTTAGTTAACGCTAAAGAAGTTCAAAAAG-3'
A217VR	5'-CTTTTTGAACTTCTTTAGCGTTAACTAAAGAATGAACGAG-3'
N218AF	5'-CGTTCATTCTTTAGCTGCGGCTAAAGAAGTTC-3'
N218AR	5'-GAACTTCTTTAGCCGCAGCTAAAGAATGAACG-3'
N218DF	5'-CGTTCATTCTTTAGCTGATGCTAAAGAAGTTC-3'
N218DR	5'-GAACTTCTTTAGCATCAGCTAAAGAATGAACG-3'
M281AF	5'-GGCTATGGTGGAGGTGCGTCGAGCGCTAAAGCTG-3'
M281AR	5'-CAGCTTTAGCGCTCGACGCACCTCCACCATAGCC-3'
M281TF	5'-GGCTATGGTGGAGGTACCTCGAGCGCTAAAGCTG-3'
M281TR	5'-CAGCTTTAGCGCTCGAGGTACCTCCACCATAGCC-3'
F368AF	5'-GCTAGCCAAAATTATACAGCGATAGATTATGCAATAGAG-3'
F368AR	5'-CTCTATTGCATAATCTATCGCTGTATAATTTTGGCTAGC-3'
F368IF	5'-GCTAGCCAAAATTATACAATTATAGATTATGCAATAGAG-3'
F368IR	5'-CTCTATTGCATAATCTATAATTGTATAATTTTGGCTAGC-3'

The mutation sites have been underlined.

Table 2

Kinetic constants for NADH and crotonoyl-CoA with respect to wild-type and mutant PfENR

	k_{cat} (s^{-1})	K_m (μM) (Crotonoyl-CoA)	K_m (μM) (NADH)
Wild-type	1.62 (±0.06)	160 ± 5	33 ± 3
A217V	1.2 (±0.02)	150 ± 4	28 ± 4.2
A217G	0.9 (±0.1)	173 ± 6	35 ± 2.2
N218A		152 ± 4	73 ± 5
N218D	1.5 (±0.07)	165 ± 7	100 ± 10
M281A		168 ± 5	39 ± 4
M281T	1.1 (±0.07)	155 ± 3.4	25 ± 12
F368A		152 ± 6	31 ± 3
F368I	1.05 (±0.15)	147 ± 2	35 ± 14

Table 3

Inhibition constants (K_i) for triclosan binding to wild-type and mutant PfENR

Enzyme	Inhibition constant (K_i) (nM)
Wild-type	0.03 (± 0.001)
A217V	232.0 (±5.0)
A217G	0.57 (±0.05)
N218A	2.10 (±0.10)
N218D	1.50 (±0.04)
M281A	9.34 (±0.81)
M281T	10.0 (±0.89)
F368A	7.20 (±0.90)
F368I	6.30 (±0.56)

Figure Legends

Figure 1 Schematic representation of the triclosan binding pocket of *P. falciparum* ENR. Triclosan and NAD^+ are shown in black. The residues mutated in the present study are shown in dark grey. The figure was generated in WebLab ViewerLite and rendered using POV-Ray.

Figure 2 Inhibition of A217V (A) and A217G (B) PfENR mutants by triclosan. Plot of apparent inhibition constant (K_i') versus NAD^+ concentration fits best to uncompetitive inhibition (solid line) with a K_i of 232 (±5) nM and 0.57 (±0.05) nM for A217V and A217G, respectively. Best fits for competitive (dashed line) and noncompetitive (dotted line) are also shown.

Figure 3 Multiple sequence alignment of ENR from *P. falciparum* (Ac. No. AF332608) with ENR from *B. napus* (Ac. No. P80030), *E. coli* (Ac. No. P29132), *M. tuberculosis* (Ac. No. P46533. The residues mutated in the present study are shown by *. Color scheme: Conserved residues shown in bold with black background, negative residues indicated by -, positive by +, aliphatic by l, aromatic by a, tiny by t, small by s, big by b, charged by c, polar by p and hydrophobic by h (all below the alignment). The figure was generated using CHROMA [24].

Figure 4 Structure of triclosan showing the ring A and B.

Biochemical Journal Immediate Publication. Published on 13 May 2004 as manuscript BJ20040302

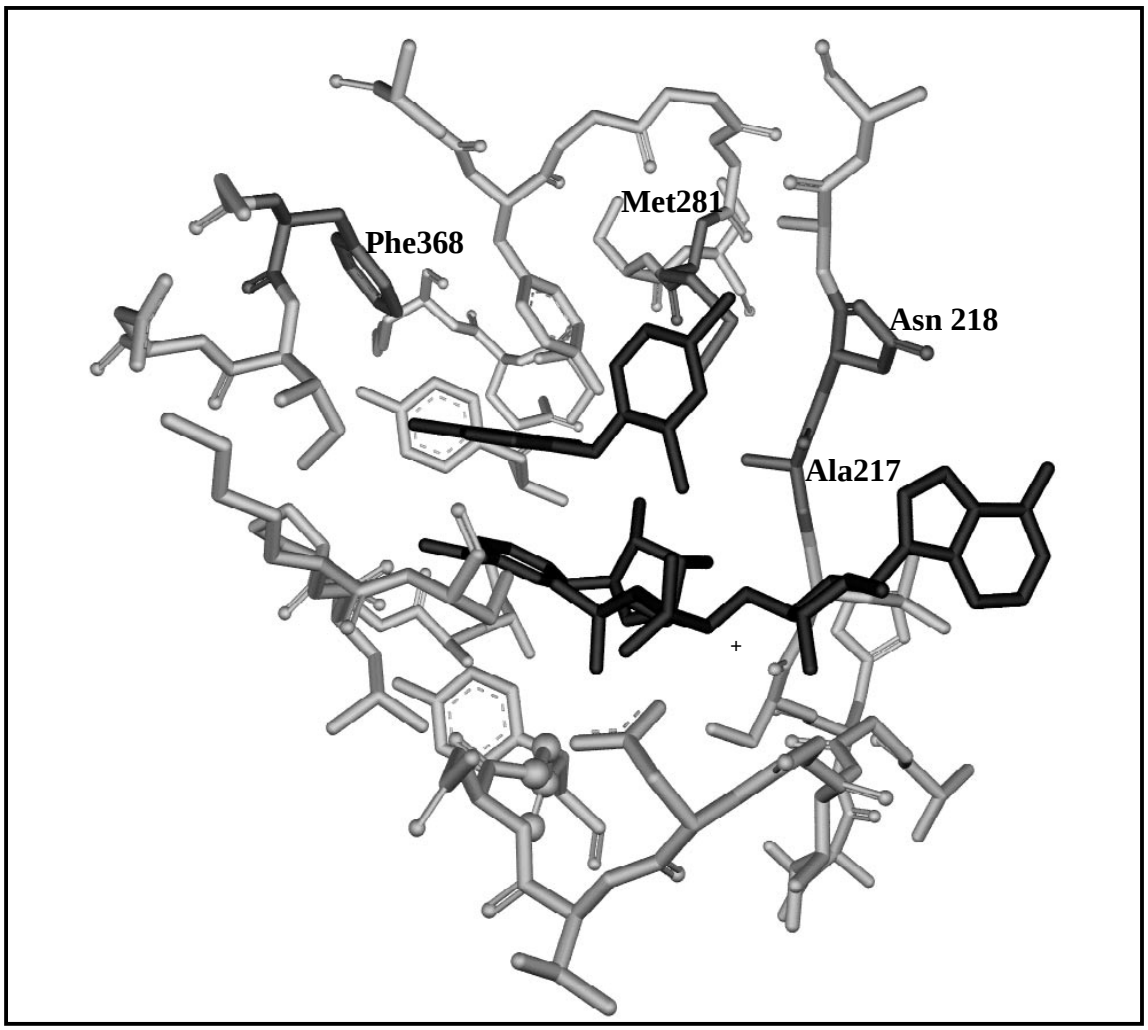

Figure 1

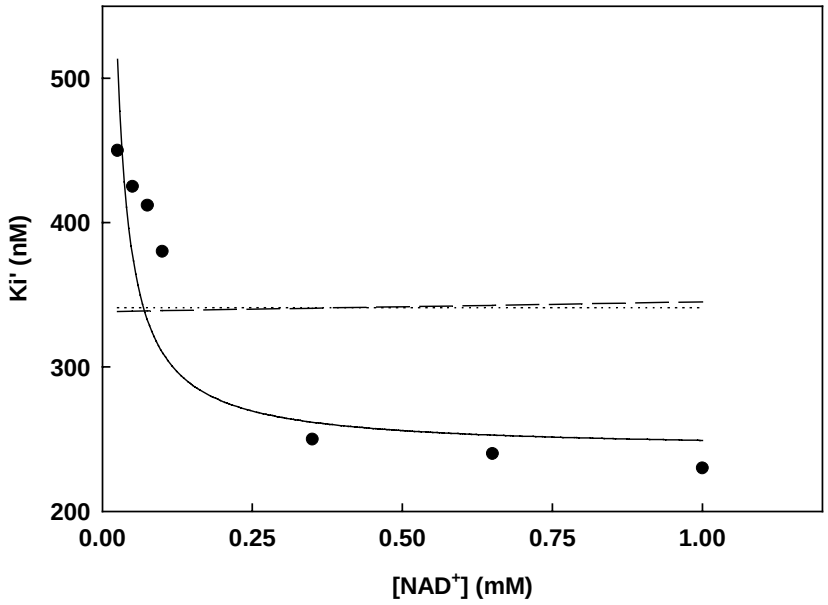

Figure 2A

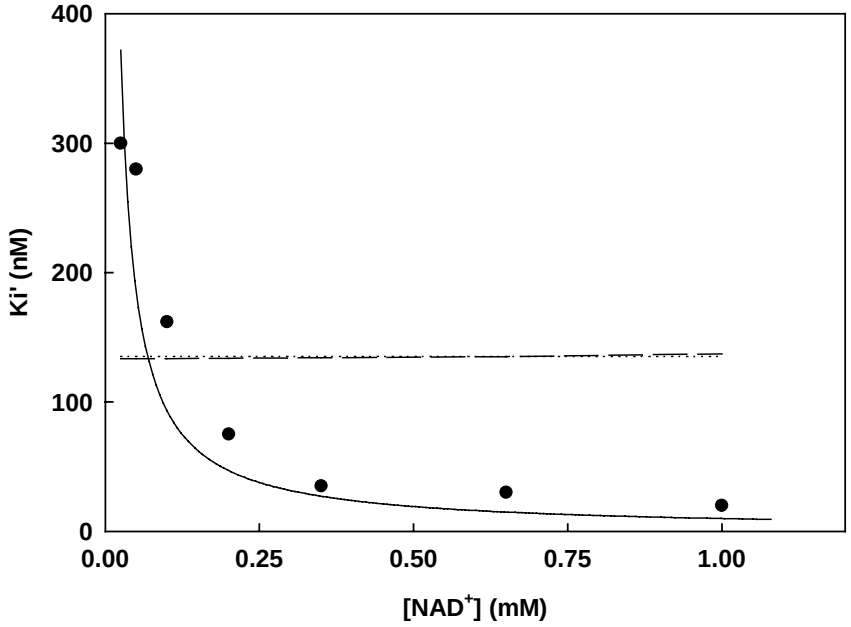

Figure 2B

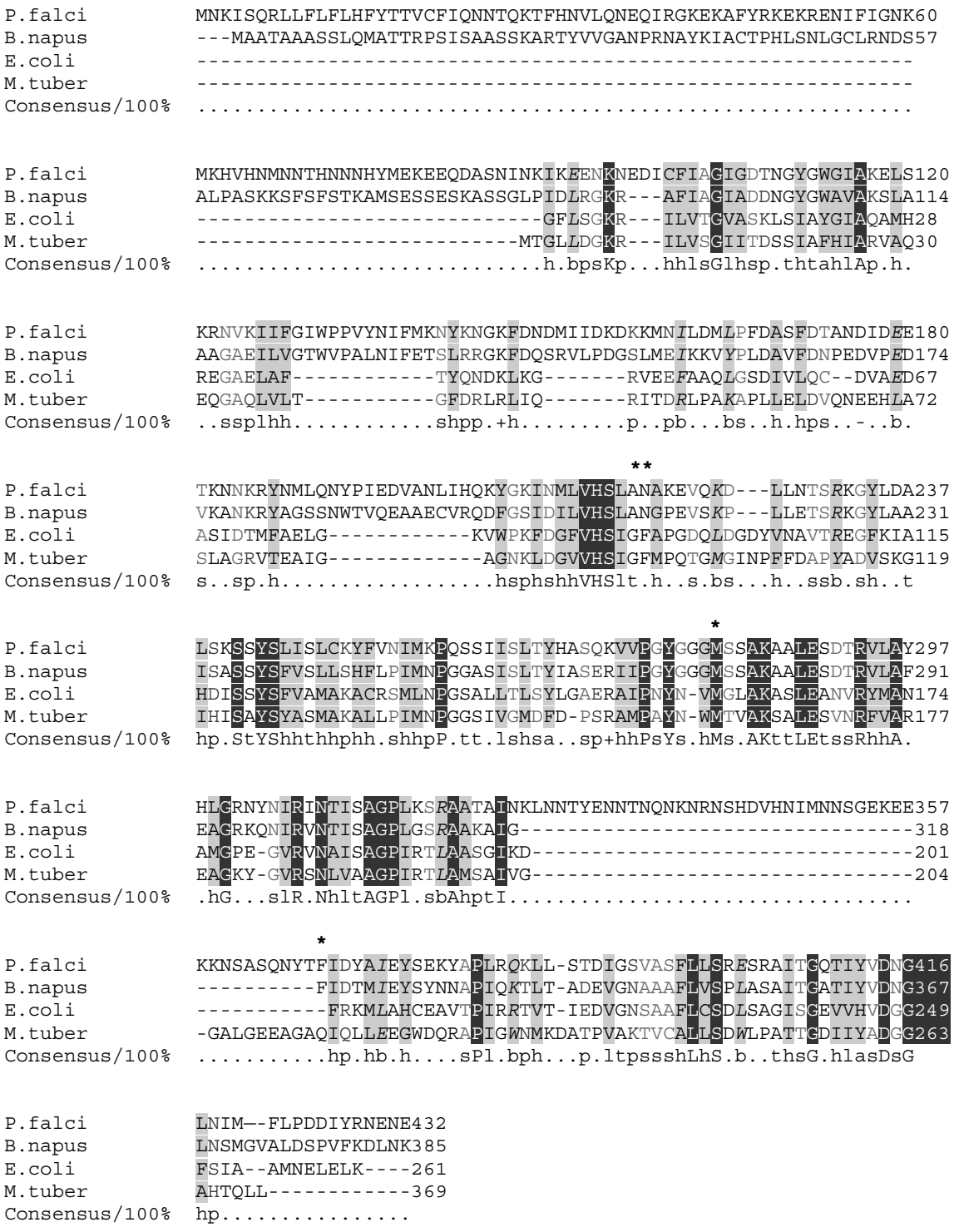

Figure 3

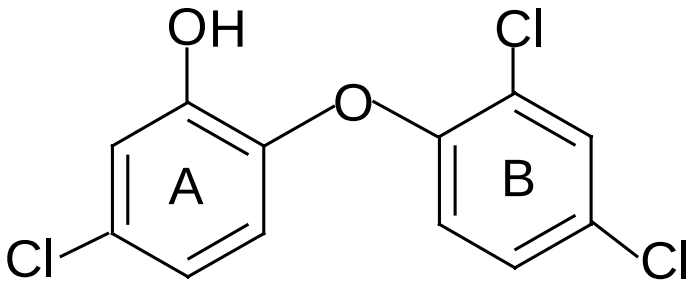

Figure 4